Pergamon

Ann. occup. Hyg., Vol 39, No 3, pp. 277–289, 1995
Elsevier Science Ltd

0003–4878/95 $9.50+0.00

0003–4878(94)00123–5

COMPUTATIONAL SIMULATION OF WORKER EXPOSURE USING A PARTICLE TRAJECTORY METHOD

Michael R. Flynn,* Ming-Ming Chen,* Taehyeung Kim† and Premkumar Muthedath*

*Department of Environmental Sciences and Engineering, University of North Carolina at Chapel Hill, Chapel Hill, NC 27599-7400, U.S.A.; and †Department of Environmental Engineering, Changwon National University, Changwon, Keungsangnam-Do, 641-240, South Korea

(*Received in final form* 9 *August* 1994)

Abstract—The velocity field downstream of a worker is approximated with a discrete vortex algorithm. This information is used to calculate trajectories of massless tracer 'particles' released from a point-source of contaminant. Concentrations in the plane of this source are estimated by averaging over a number of such trajectories. Approximations include: (1) representing the worker by a two-dimensional elliptical cylinder; and (2) representing tracer gas contaminant by massless particles generated without momentum. These particles are transported by both vortex shedding and turbulent diffusion. Computer-predicted mean concentrations in the near-wake region downstream of the worker compare well with results from wind-tunnel tracer gas experiments employing a mannequin. Subsequently, the concept of a computational breathing zone is introduced, and predictions of worker exposure are made. These simulations of time-integrated breathing zone concentration also compare well with measured values.

INTRODUCTION

One of the most significant aspects of contaminant dispersion in the vicinity of a worker is the tendency for the contaminant to recirculate. As air flows around the worker, boundary layer separation produces counter-rotating eddies on the downstream side of the body. These eddies or vortices can transport contaminant into the breathing zone, and reduce the effectiveness of any intended ventilation. Theoretical and experimental studies (Ljungqvist, 1979; George *et al.*, 1990; Tum Suden *et al.*, 1990; Flynn and Miller, 1991; Kim and Flynn, 1991a,b), as well as field observations (Heriot and Wilkinson, 1979), call attention to the importance of this effect in determining worker exposure.

To predict exposure, and evaluate the potential benefit from any intended control intervention, a mathematical model capable of simulating boundary layer separation around a worker was developed (Flynn and Miller, 1991). The model employs a computational technique known as the discrete vortex method (DVM) for the solution of the incompressible Navier–Stokes equations in vorticity transport form. It provides a two-dimensional prediction of the time-dependent velocity field around a worker (modelled as a cylinder of elliptic cross-section) immersed in a uniform freestream. This estimated velocity field was used to predict the average concentration near the worker based on the assumption of contaminant transport by vortex shedding exclusively. Transport by turbulent diffusion at scales smaller than the eddies captured in the computational simulation was not considered in that work.

The objective of this research is to expand the model, solve the advective–dispersive

equation, and obtain estimates of the spatial and temporal concentration field in the plane of a fixed point-source downstream of the worker. This information is then used to extend the work and make predictions of time-averaged breathing zone concentration. A procedure (Turfus, 1988) is employed to capture turbulent transport at scales smaller than those resolved by the DVM program. An important issue is the limitation of a two-dimensional simulation in providing predictions of this three-dimensional phenomenon. Computational estimates of concentration are compared with measured values taken in wind tunnel studies employing a mannequin.

THEORY

The transport of a passive scalar, such as neutrally buoyant tracer gas in an air flow field, is governed by the advective–dispersive equation:

$$\frac{\partial C}{\partial t} + \mathbf{U} \cdot \nabla C = \nabla \cdot (\Gamma \nabla C), \tag{1}$$

where C is the tracer concentration, $\mathbf{U}$ is the velocity field, t is time and Γ is a turbulent diffusion coefficient. The time-dependent air velocity field around a worker is governed by the incompressible continuity and Navier–Stokes equations:

$$\nabla \cdot \mathbf{U} = 0 \tag{2}$$

$$\frac{\partial \mathbf{U}}{\partial t} + \mathbf{U} \cdot \nabla \mathbf{U} = \nu \nabla^2 \mathbf{U} - \nabla P, \tag{3}$$

where P is the dynamic pressure and ν is the kinematic viscosity. The standard Cartesian co-ordinate representation of the velocity field is:

$$\mathbf{U} = u\hat{i} + v\hat{j} + w\hat{k} \tag{4}$$

here u, v and w are the x, y and z velocity components, respectively. In this work the origin of the co-ordinate system is the geometric centre of the ellipse representing the worker, and the x direction is perpendicular to the freestream direction, see Fig. 1.

In the case of two-dimensional flow the Navier–Stokes equations can be written in vorticity transport form with pressure conveniently eliminated:

$$\frac{\partial \omega}{\partial t} + \mathbf{U} \cdot \nabla \omega = \nu \nabla^2 \omega \tag{5}$$

here ω, the vorticity, is the curl of the velocity field, for flow in the x–y plane:

$$\omega = \frac{\partial v}{\partial x} - \frac{\partial u}{\partial y}. \tag{6}$$

NUMERICAL METHODS

The time-dependent air flow around the worker (cylinder), is computed by approximating solutions to Equations (2) and (5) with the discrete vortex code described in Flynn and Miller (1991). The code is improved here by employing the fast-multipole algorithm developed by Greengard and Rokhlin (1987) to speed up vortex calculations. In addition, a boundary integral method is employed for the potential

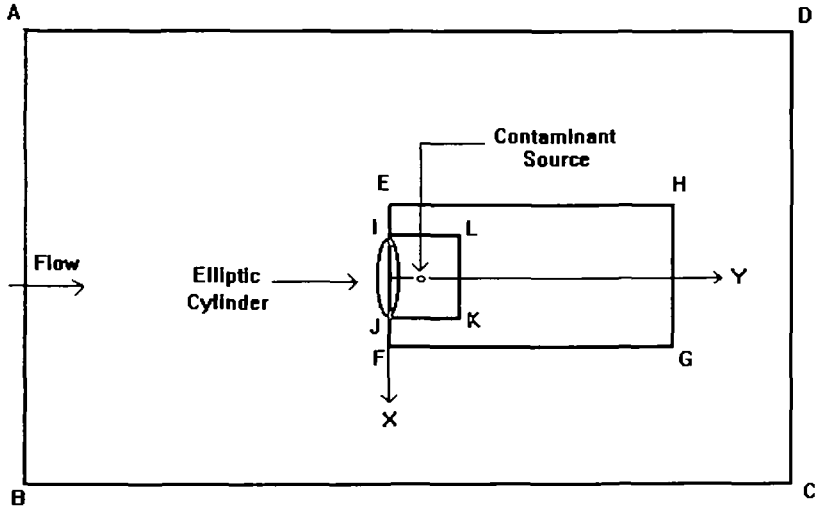

ABCD Flow Domain
EFGH Concentration Domain
IJKL Computational Breathing Zone

Fig 1. The computational domain

flow calculation. The output of the program is the time evolving velocity field needed to solve Equation (1) and provide an estimate of the spatio-temporal concentration field.

Figure 1 shows the flow domain, rectangle ABCD. It is the region within which velocity is calculated. The Cartesian co-ordinates are: A(−100, −100); B(100, −100); C(100, 100) and D(−100, 100). The concentration domain, rectangle EFGH, defines a zone for the calculation of concentration. The co-ordinates are: E(−7.5, 0); F(7.5, 0); G(7.5, 18); and H(−7.5, 18). Finally, the computational breathing zone is defined by rectangle IJKL. This region was selected to average concentrations for comparison to breathing zone measurements. The co-ordinates are I(−1.25, 0); J(1.25, 0); K(1.25, 2.75) and L(−1.25, 2.75).

Solution of Equation (1) is obtained by assuming that the small-scale diffusivity, Γ, is constant in both space and time. A Lagrangian particle-tracking algorithm is employed to calculate concentrations in the plane of a point source located downstream of the worker (elliptical cylinder) by using a time-dependent particle weighting factor (Turfus, 1988). Dispersion of contaminant in time is simulated by calculating trajectories for a number of massless 'particles' released into the flow. Mean concentrations are predicted by imposing a uniform grid of cells on a sub-domain of the wake region (see Fig. 2) and averaging the number of particles in each cell over time. This sub-domain is slightly larger than the computational breathing zone and was selected to examine equilibrium conditions in the vicinity of the worker.

Trajectory calculations

The DVM used to calculate the air velocity field, employs a fractional step method (Bui and Oppenheim, 1987) to split the vorticity–transport equation into Euler's equation and the diffusion equation, respectively:

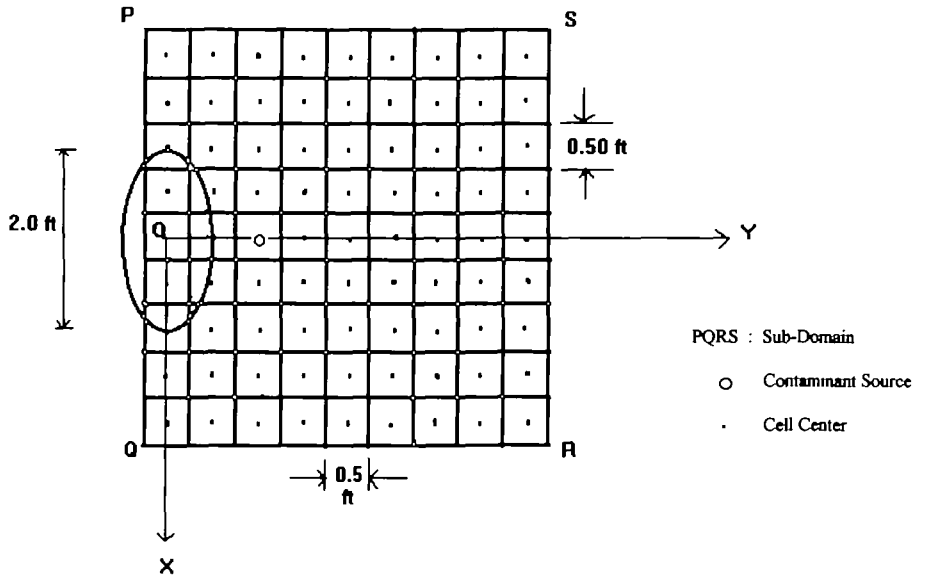

Fig. 2. Computational concentration cells in the plane of the point source

$$\frac{\partial \omega}{\partial t} + \mathbf{U} \cdot \nabla \omega = 0 \tag{7}$$

$$\frac{\partial \omega}{\partial t} = \nu \nabla^2 \omega. \tag{8}$$

The solution for Euler's equation depends upon a theorem (Batchelor, 1967) that guarantees an incompressible velocity field may be decomposed into the sum of a potential and a rotational flow. The solution (Bui and Oppenheim, 1987) for the diffusion equation, with an impulse initial condition, is a Gaussian distribution of zero mean and variance:

$$\sigma_\omega^2 = 2\nu\Delta t, \tag{9}$$

where σ_ω is the standard deviation of a given vortex element displacement and Δt is a finite interval of time. A random walk algorithm is used to obtain the solution of the diffusion equation.

With a constant small-scale contaminant diffusivity, Γ, the advective–dispersive equation is also split into Euler's equation and a diffusion equation:

$$\frac{\partial C}{\partial t} + \mathbf{U} \cdot \nabla C = 0 \tag{10}$$

$$\frac{\partial C}{\partial t} = \Gamma \nabla^2 C. \tag{11}$$

Concentration particles are generated without momentum, their movement is affected by convection from the vortex elements, and small-scale diffusion. Concentration particles move according to the equations:

$$x_{n+1} = x_n + u_n(\Delta t) + \eta_1 \tag{12}$$

and

$$y_{n+1} = y_n + v_n(\Delta t) + \eta_2, \tag{13}$$

where Δt is a finite interval of time, and the n subscript refers to the time step. The variables η_1 and η_2 are independent random variables drawn from a Gaussian distribution of zero mean, and variance, σ_C^2, equal to $2\Gamma\Delta t$.

The trajectory algorithm splits the movement of a concentration particle into a diffusion step with one half the variance, a convective step, and finally another diffusion step, again with one half the variance. This improves the accuracy of the fractional step method (Tiemroth, 1986; Bui and Oppenheim, 1987).

The magnitude of the small-scale diffusivity is assigned somewhat arbitrarily. Turfus (1988) shows a method for estimating it which is applied here without modification. Γ is the product of a length scale (l_e) and a velocity scale (u_e). The length scale is selected as the vortex blob cut-off radius, for the simulations conducted here $l_e = 36.4$ cm (0.077 ft). The velocity scale is calculated with the assumption that the turbulence intensity is 10% and the ratio of u_e to the rms velocity fluctuation is 0.145; this is based on several other assumptions as outlined by Turfus (1988).

Concentration calculations

The main purpose of this research is to predict concentration resulting from a point source with a constant generation rate. Concentration particles are released, 10 per time-step, from a fixed point, at a location designed to mimic a typical hand-held source. They move under the influence of the flow field, according to Equations (12) and (13). These particles are removed when they cross the removal boundary (RB). RB is set at $y = 5.5$ m (18 ft), beyond this boundary simulations suggest the probability of a particle being recirculated back to the near-wake region is essentially zero.

Turfus (1988) provides a description relating concentration to the particle positions: "After a given time, the distribution of particles in the flow reaches a statistical equilibrium, i.e. the expected number of particles in any given region at a single time-step does not tend to increase or decrease with time. By the ergodic theorem (Panchev, 1971), if the distribution of particles were statistically stationary throughout this time period and the average number of particles in each cell at each time-step had therefore converged to a number independent of time, then we could equate this number to the ensemble mean concentration (due to a line-source of strength $Q_s = N$ particles/Δt) integrated over the cell".

Turfus (1988) presents a method for estimating concentration from point and line sources in two-dimensional flow. For a line-source, the mean concentration, $\bar{C}$ can be expressed as a dimensionless group χ_{2d} by the following transform:

$$\chi_{2d} = \frac{\bar{C} U_\infty D}{Q_s}, \tag{14}$$

where U_∞ is the freestream velocity, Q_s is the two-dimensional source strength, and D is the mannequin width perpendicular to the free stream.

By imposing a uniform grid over the computational domain with square cells of length $S(D)$, where S is a fraction, then if N_{ij} is the mean number of particles in a cell

with centre (x_i, y_j), the dimensionless mean concentration within this cell is approximated as:

$$\chi_{2d} = \frac{N_{ij} U_\infty \Delta t}{(S^2 D) N}, \tag{15}$$

N is the number of particles generated per time-step (Turfus, 1988).

A similar analysis is presented (Turfus, 1988) for calculating concentration fields in the plane of a point-source, in a two-dimensional flow, by including a weighting factor inversely proportional to the age of the particle (i.e. the time since the particle is released). Thus, the dimensionless mean concentration for a point-source, χ_{3d}, is:

$$\chi_{3d} = \frac{\overline{C(x_i, y_i z = 0)} U_\infty D^2}{Q_s}, \tag{16}$$

where Q_s is the contaminant source flow in cfm. Equation (15) can be modified to account for the point source as:

$$\chi_{3d} = \frac{N^*_{ij} U_\infty \Delta t}{(S^2 D) N}, \tag{17}$$

where N^*_{ij} is the number of weighted tracer particles in the ij cell. Equation (17) is used to approximate the concentration field in the plane of the point source by weighting the contribution of each particle with a factor, $f(t)$, where

$$f(t) = \frac{1}{[\sigma_z^2(t) 2\pi]^{1/2}} \tag{18}$$

and

$$\sigma_z^2(t) = \delta^2 + 2\sigma_w^2 T_L^2 \left(1 - e^{(-t/T_L)} + \frac{t}{T_L} \right), \tag{19}$$

$\sigma_z^2(t)$ is the particle variance in the z direction, t is the dimensionless age of the particle, T_L is the Lagrangian integral time scale based on the streamwise velocity fluctuations, δ is a small distance to avoid singularity in the formulation (set here as 0.01), and σ_w^2 is the velocity variance out of the plane of simulation (i.e. the square of the z-velocity fluctuation). σ_w^2 is calculated assuming a 10% overall turbulence intensity. A dimensionless value for T_L of 0.58 was suggested by Turfus (1988). In the work conducted here T_L was subjected to a sensitivity analysis and used as a calibration factor to tune the model with experimental data. After calibration the model was strained by examining conditions outside the calibration range.

EXPERIMENTAL METHODS

The ultimate objective of the modelling effort is to develop algorithms for estimating worker exposure. The flow of air around a worker in a uniform freestream has been studied extensively by Kim and Flynn (1991a, b) with wind tunnel simulations employing a mannequin and the concept of Reynolds number similarity. Flow visualization work indicates that while vortex shedding does exist, complex three-dimensional flow patterns are also present, and a two-dimensional computation

Table 1. Summary of numerical simulations

	Velocity (ft min^{-1})	Strouhal number	Time step (min)	Concentration (ppm)
I	50	0.21	0.0020	42.0
II	50	0.21	0.0020	13.2
III	33 3	0.19	0.0025	17.2
IV	83.3	0 20	0.0015	9.0

will be somewhat limited. Nevertheless, the cost of three-dimensional simulations is substantial, and in an effort to examine the limitations of the approach outlined here, experimental data from Kim and Flynn (1991b) are used to examine the numerical predictions.

A wind tunnel of 1.524 m (5 ft) square cross-section was operated at freestream velocities of 0.51, 0.76 and 1.27 m s^{-1} (100, 150, 250 ft min^{-1}). A mannequin 1.04 m (41 in.) tall and 20.3 cm (8 in.) wide at the chest was placed in the flow facing downstream. A small 0.635 cm (0.25 in.) dia. ceramic diffuser was placed in the hands of the mannequin, and neutrally buoyant 10% sulphur hexafluoride tracer gas was metered through it at a flow of 2.36×10^{-6} m^3 s^{-1} (0.005 ft^3 min^{-1}). Concentrations were measured at locations downstream of the mannequin approximately in the plane of the source (chest level) and in other planes (Kim and Flynn, 1991b). Each sampling location was 10.15 cm (4 in.) away from its nearest neighbour. In addition, measurements of breathing zone concentration were taken from the mouth of the mannequin. SF_6 concentration was measured using a calibrated i.r. spectrophotometer sampling at 1.0 l. min^{-1}. Sampling was conducted for a 5 min period after allowing the flow 15 min to achieve an equilibrium.

RESULTS

Numerical simulations conducted here represent flow of air around a worker by modelling him or her as a two-dimensional elliptical cylinder. The cylinder is 0.61 m (2.0 ft) wide, by 0.31 m (1.0 ft) deep, and the point-source of contaminant is at the co-ordinates (0.0 ft, 1.0 ft). Free stream velocities in the simulations were selected to produce the same Reynolds numbers as those around the mannequin used in the wind tunnel study (Kim and Flynn, 1991b) for comparison. Four numerical simulations (I–IV) were run. Table 1 presents a summary of these simulations. The first two simulations were used to calibrate the model; the remaining two were conducted to examine the ability of the model to operate outside the range of calibration.

After 15 time steps, concentration particles were released into the two-dimensional flow field. The time needed for the concentration field in simulation I to reach statistical equilibrium is presented in Fig. 3. This shows the development of concentration with time in the sub-domain $-0.69\text{ m} < x < 0.69\text{ m}$ $(-2.25\text{ ft} < x < 2.25\text{ ft})$ and $0\text{ m} < y < 1.30\text{ m}$ $(-0.25\text{ ft} < y < 4.25\text{ ft})$ as well as in the concentration domain $-2.3\text{ m} < x < 2.3\text{ m}$ $(-7.5\text{ ft} < x < 7.5\text{ ft})$ and $0\text{ m} < y < 5.5\text{ m}$ (18 ft). After a transient phase of about 200 time steps in the sub-domain, and 300 time steps in the concentration domain, the total particle weights (i.e. concentration) approaches equilibrium. The simulations were continued for a total of 800 time steps to calculate

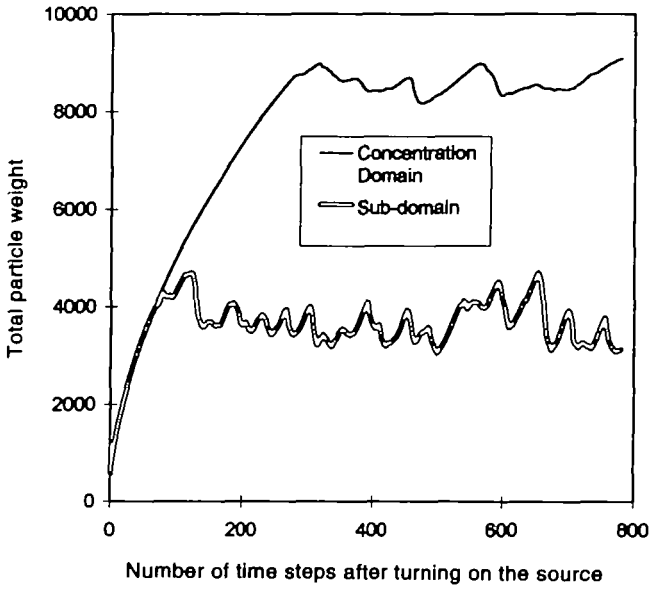

Fig. 3. Total particle weights as a function of time step for simulation I.

the mean concentrations. The concentrations reported here are obtained by averaging over approximately 500–600 time steps after equilibrium in the global domain has been achieved.

In addition to concentration, velocity fields were time-averaged as well. Figure 4 presents a vector plot of an instantaneous velocity field taken from simulation IV, while Fig. 5 presents the velocity field for the same simulation only averaged over 800 time steps. Surprisingly the time-averaged velocity field shows little recirculation, indeed the anticipated result of two counter-rotating eddies was not realized. However, Strouhal numbers were well predicted in all cases (see Table 1).

Computer-predicted mean concentration contours resulting from simulation I are presented in Fig. 6 for $T_L = 0.2$. This value for T_L was selected to provide good agreement with the spatial average reported by Kim and Flynn (1991b) for the plane at the mannequin's chest level. In other words by averaging the numerically predicted concentrations over a region comparable to the experimental scale, and adjusting T_L to provide good agreement, a preliminary calibration of the model was effected. It is encouraging to note the close agreement between this value and Turfus' value of 0.58, as well as the symmetric nature of the contours. The numerically predicted average concentration was 42.0 ppm while the comparable measured values were 36.7 and 47.2 ppm taken in two separate replications.

At this point it was desirable to examine whether or not the model could be used to generate predictions of exposure, i.e. breathing zone concentrations integrated over time. A computational breathing zone was selected as the downstream region $-0.38\text{ m} < x < 0.38\text{ m}$ ($-1.25\text{ ft} < x < 1.25\text{ ft}$) and $0\text{ m} < y < 0.84\text{ m}$ ($0\text{ ft} < y < 2.75\text{ ft}$). This was based on the concept that the formation region for vortex shedding is on the order of a body dimension. The numerically predicted concentration (simulation II) in this region at 50 ft min^{-1} with $T_L = 10.0$ was 12.0 ppm while the measured breathing

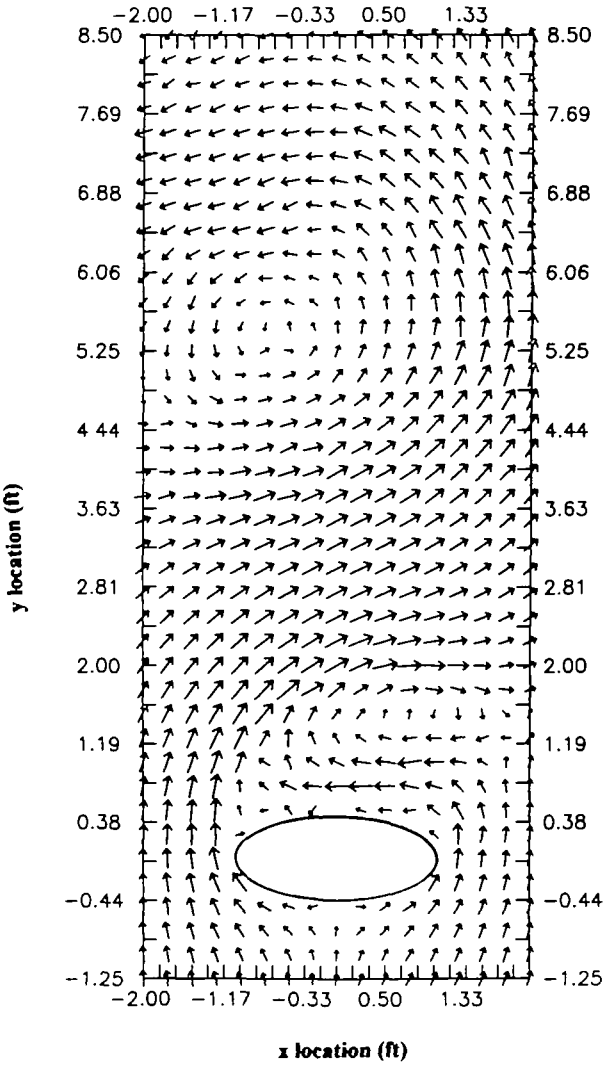

Fig. 4 The instantaneous velocity field from simulation IV after 500 time steps.

zone concentrations (Kim and Flynn, 1991b) were 9.78 and 14.22 ppm for the same conditions. Subsequently the value for T_L was kept at 10 and simulations III and IV were run at 33.3 and 83.3 ft min^{-1}, excellent agreement with measured values of breathing zone concentration were obtained (see Table 2).

Note that to maintain Reynolds number similarity different values of velocity are used in the numerical simulation than those in the experiment. Appropriate dimensionless variables are used to calculate concentrations which are then rescaled to experimental values for comparison. These simulations were run on a Convex supercomputer and took a total of about 5 h of CPU time for 800 time steps.

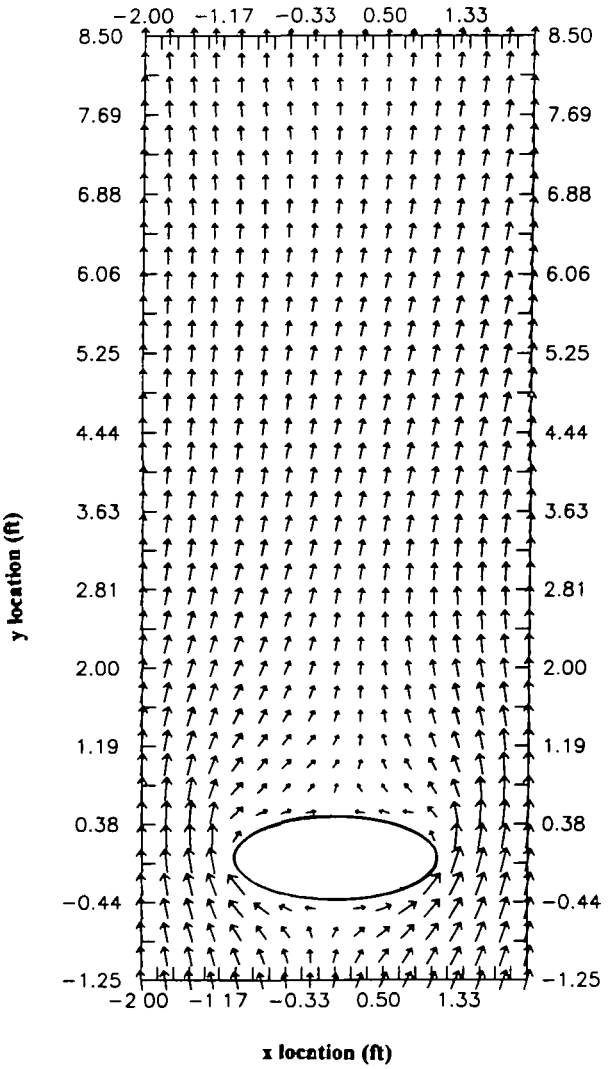

Fig. 5. The velocity field for simulation IV averaged over 800 time steps.

DISCUSSION

Mean concentrations predicted in a two-dimensional flow field by using a particle trajectory algorithm, are determined by three major factors: (1) the time-dependent velocity field characterized by periodic vortex shedding; (2) the weighting factor, $f(t)$, which accounts for the probability of contaminant particles leaving the source plane; and (3) the small-scale diffusivity, Γ, which tends to spread the contaminant particles out in the plane of simulation.

In high Reynolds number convection-dominated flows (such as are of concern in occupational exposures) the velocity field is of most concern, and the periodic nature of vortex shedding is critical. A numerical simulation must be able to capture this phenomenon if reasonable estimates of exposure are desired. The two important pieces

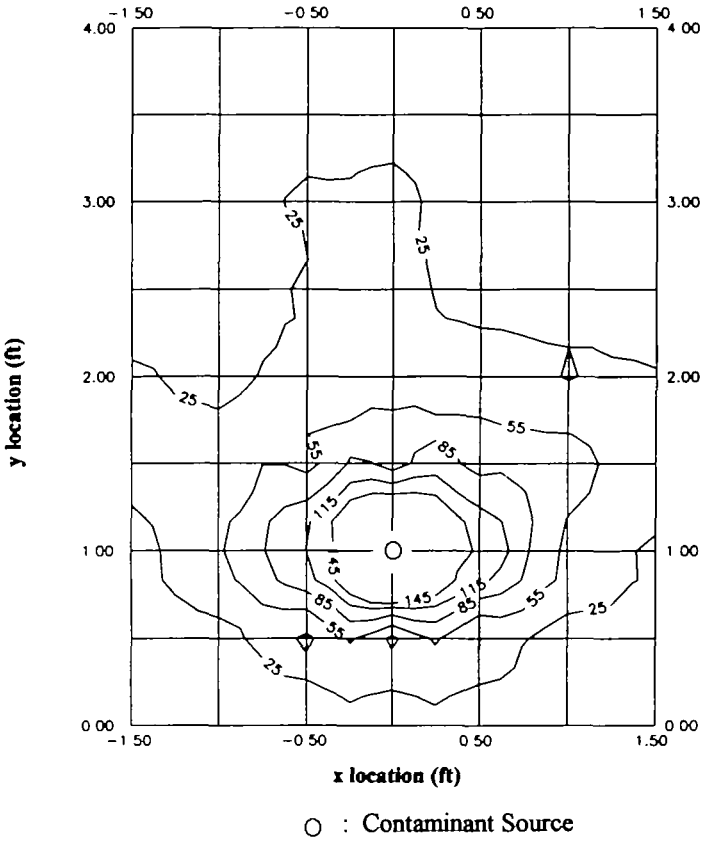

Fig. 6. Concentration contours from simulation I.

Table 2. Comparison of predicted and experimental breathing zone concentrations

Experimental velocity (ft min^{-1})	Average measured breathing zone concentration* (ppm)	Average predicted breathing zone concentration (ppm)
100	19.5 (17.0, 22.0)	17.2
150	12.0 (9.8, 14.2)	13.21
250	7.2 (8.3, 6.1)	9 04

*Values in parentheses indicate 1 SD Experimental values from Kim and Flynn (1991b).

of information are the shedding frequency, i.e. Strouhal number, and the eddy size. Our simulations capture the Strouhal number quite well over a range of Reynolds numbers, however the eddy shape and size may not be simulated quite so well. The time averaged velocity fields do not indicate the counter rotating eddies downstream of the ellipse that we might anticipate.

This may be due to the fact that after the eddies begin to shed they tend to grow over the whole length of the ellipse rather than preferentially occupying one side, see Fig. 3, which illustrates an eddy about to be shed growing along the length of the ellipse. This may be due to errors in approximating the geometry as well as in long-time integration errors which are associated with these types of calculations.

Despite the limitations, reasonable concentrations are possible not only for the plane of the source, but the breathing zone as well. Using a value for T_L of 10.0 and averaging over the computational breathing zone, produces excellent agreement with measurements of breathing zone concentrations obtained using a mannequin. The ability to average over the smaller region close to the cylinder means that faster, more economic simulations are possible. Indeed averaged values for 400–600 time steps produced results quite comparable to the longer averages.

Despite the rather limited nature of this simulation velocity fields, worker motion, and even hood flows can be incorporated into the approach. A recent article (Kim and Flynn, 1991a) incorporates multiple objects and examines the impact of worker position on the air velocity field.

CONCLUSION

The design of control interventions to reduce worker exposure to toxic airborne pollutants is hampered by the lack of a model to predict exposure as a function of appropriate variables. Two of the most important predictors of exposure are the contaminant generation rate and the air flow field in the vicinity of the worker. If the worker's breathing zone concentration as a function of time can be estimated before control equipment, e.g. local exhaust ventilation, is installed, then the probability of it being successful can be evaluated prior to its construction. The extra cost of over-control can be eliminated, and the optimal design implemented.

In addition, a model capable of examining work practices, i.e. worker activity level, orientation with respect to airflow, etc., would have the capability to evaluate the relative effectiveness of alternate control strategies. For example, in some cases it may be that increasing air flow will result in only minimal reduction in exposure (possibly an increase?), whereas changing how the job is done, i.e. worker orientation with respect to the flow, may prove a more effective intervention.

The equations governing the flow of air around the worker and the transport of contaminant in such a field are well known. The discrete vortex method is an effective tool for capturing the vortex shedding responsible for contaminant transport when a worker is immersed in a uniform freestream. A particle trajectory procedure outlined by Turfus (1988) for solution of the advective–dispersive equation is employed here to make reasonable estimates of worker exposure in this sample flow.

The method is limited in that the velocity predicted by the DVM is two-dimensional and the flow around a worker is truly a three-dimensional phenomenon. Results presented here suggest that by selection of the appropriate Lagrangian time scale (T_L),

and by averaging over an appropriate computational breathing zone, this drawback can be minimized.

Acknowledgements—This work was supported by funding from the National Institute of Occupational Safety and Health grant 5 R01 OH02858. The authors also wish to thank Dr L. Greengard for providing the multipole subroutines, and for the support provided by Convex Computers.

REFERENCES

Batchelor, G. K. (1967) *An Introduction to Fluid Dynamics*. Cambridge University Press, Cambridge, U.K.

Bui, T. D. and Oppenheim, A. K (1987) Evaluation of wind effects on model buildings by the random vortex method. *Appl. Numer. Math.* **3,** 195–207.

Flynn, M. R. and Miller, C. T. (1991) Discrete vortex methods for the simulation of boundary layer separation effects on worker exposure. *Ann. occup Hyg.* **35,** 35–50.

George, D., Flynn, M. R. and Goodman, R. (1990) The impact of boundary layer separation on local exhaust design and worker exposure. *Appl. occup. Environ. Hyg.* **5,** 501–509.

Greengard, L. and Rokhlin, V. (1987) The rapid evaluation of potential fields in three dimensions. In *Lecture Notes in Mathematics—Vortex Methods*. Springer, Berlin.

Heriot, N. R. and Wilkinson, J. (1979) Laminar flow booth for the conytrol of dust. *Filtration Separ.* March–April, 159–174.

Hiller, R. and Cherry, N. J. (1981) The effects of stream turbulence on separation bubbles. *J. Wind Engng ind. Aerodyn.* **8,** 49–58.

Hinze, J. O (1975) *Turbulence* (2nd Edn), pp. 48–58. McGraw-Hill, New York.

Kim, T. and Flynn, M. R. (1991a) Airflow pattern around a worker in a uniform freestream. *Am ind. Hyg. Ass. J.* **52,** 287–296.

Kim, T. and Flynn, M. R. (1991b) Modeling a worker's exposure from a hand-held source in a uniform freestream. *Am. ind. Hyg. Ass. J.* **52,** 458–463.

Ljungqvist, B. (1979) Some observations on the interaction between air movements and the dispersion of pollution. Document D8: 1979. Swedish Council for Building Research, Stockholm, Sweden.

Panchev, S. (1971) *Random Function and Turbulence*. Pergamon Press, Oxford.

Tiemroth, E. C. (1986) The simulation of viscous flow around a cylinder by the random vortex method. Doctoral Dissertation, University of California, Berkeley.

Tum Suden, K. D., Flynn, M. R. and Goodman, R (1990) Computer simulation in the design of local exhaust hoods for shielded metal arc welding *Am. ind. Hyg. Ass. J.* **51,** 115–126.

Turfus, C. (1988) Calculating mean concentrations for steady sources in recirculating wakes by a particle trajectory method. *J. Atmos. Environ* **22,** 1271–1290.